Cambridge University Press
978-0-521-89886-7 - The Emission-Line Universe: XVIII Canary Islands Winter School of Astrophysics
Edited by Jordi Cepa
Excerpt
More information

1. What can emission lines tell us?

GRAŻYNA STASIŃSKA

1.1. Introduction

Emission lines are observed almost everywhere in the Universe, from the Earth's atmosphere (see Wyse & Gilmore 1992 for a summary) to the most-distant objects known (quasars and galaxies), on all scales and at all wavelengths, from the radio domain (e.g. Lobanov 2005) to gamma rays (e.g. Diehl *et al.* 2006). They provide very efficient tools to explore the Universe, measure the chemical composition of celestial bodies and determine the physical conditions prevailing in the regions where they are emitted.

The subject is extremely vast. Here, we will restrict ourselves in wavelength, being mostly concerned with the optical domain, with some excursions to the infrared and ultraviolet domains and, occasionally, to the X-ray region.

We will mainly deal with the mechanisms of line production and with the interpretation of line intensities in various astrophysical contexts. We will discuss neither quasars and Seyfert galaxies, since those are the subject of Chapter 5, nor Lyman-α galaxies, which are extensively covered in Chapter 4 of this book. However, we will discuss diagnostic diagrams used to distinguish active galaxies from other emission-line galaxies and will mention some topics linked with H Lyα. Most of our examples will be taken from recent literature on planetary nebulae, H II regions and emission-line galaxies. Emission-line stars are briefly described in Chapter 7 and a more detailed presentation is given in the book *The Astrophysics of Emission Line Stars* by Kogure & Leung (2007).

The vast subject of molecular emission lines has been left aside. The proceedings of the symposium *Astrochemistry: Recent Successes and Current Challenges* (Lis *et al.* 2006) give a fair introduction to this rapidly expanding field.

In the present text, we will not go into the question of Doppler shifts or line profiles, which tell us about radial velocities and thus about dynamics. This is of course a very important use of emission lines, which would deserve a book of its own. For example, for such objects as planetary nebulae and supernova remnants, emission-line profiles allow one to measure expansion velocities and thus investigate their dynamics. Determining the distribution of radial velocities of planetary nebulae in galactic haloes is a way to probe their kinematics and infer the dark-matter content of galaxies (Romanowsky 2006). Redshift surveys to map the three-dimensional distribution of galaxies in the Universe strongly rely on the use of emission lines (e.g. Lilly *et al.* 2007), which is the most-reliable way to measure redshifts.

We will, however, mention the great opportunity offered by integral-field spectroscopy at high spectral resolution, which provides line intensities and profiles at every location in a given field of view. With appropriate techniques, this allows one to recover the three-dimensional (3D) geometry of a nebula.

The purpose here is not to review all the literature on ionized nebulae, but rather to give clues for understanding the information given by emission lines, to provide some tools for interpreting one's own data, and to argue for the importance of physical arguments and common sense at each step of the interpretation process. Therefore, we will review methods rather than objects and papers. This complements in some sense the text entitled "Abundance determinations in H II regions and planetary nebulae" (Stasińska 2004), to

The Emission-Line Universe, ed. J. Cepa. Published by Cambridge University Press.

which the reader is referred. In order to save space, the topics that have been treated extensively there will not be repeated, unless we wish to present a different approach or add important new material.

In the following, we will assume that the reader is familiar with the first three sections of Stasińska (2004). We also recommend reading Ferland's outstanding (2003) review "Quantitative spectroscopy of photoionized clouds". Those wishing for a more-complete description of the main physical processes occurring in ionized nebulae should consult the textbooks *Physical Processes in the Interstellar Medium* by Spitzer (1978), *Physics of Thermal Gaseous Nebulae* by Aller (1984), *Astrophysics of the Diffuse Universe* by Dopita & Sutherland (2003) and *Astrophysics of Gaseous Nebulae and Active Galactic Nuclei* by Osterbrock & Ferland (2006). For a recent update on X-ray astrophysics, a field that is developing rapidly, one may consult the AIP Conference Proceedings on *X-ray Diagnostics of Astrophysical Plasmas: Theory, Experiment, and Observation* (Smith 2005).

1.2. Generalities

1.2.1 *Line-production mechanisms*

Emission lines arise in diffuse matter. They are produced whenever an excited atom (or ion) returns to lower-lying levels by emitting discrete photons. There are three main mechanisms that produce atoms (ions) in excited levels: recombination, collisional excitation and photoexcitation.

1.2.1.1 Recombination

Roughly two thirds of the recombinations of an ion occur onto excited states from which de-excitation proceeds by cascades down to the ground state. The resulting emission lines are called recombination lines and are labelled with the name of the *recombined* ion, although their intensities are proportional to the abundance of the *recombining* species. The most-famous (and most commonly detected) ones are H I lines (from the Balmer, Paschen, etc. series), which arise from recombination of H^+ ions; He I lines ($\lambda 5876, \ldots$), which arise from recombination of He^+; and He II lines ($\lambda 4686, \ldots$), which arise from recombination of He^{++} ions. Recombination lines from heavier elements are detected as well (e.g. C II $\lambda 4267$, O II $\lambda 4651, \ldots$), but they are weaker than recombination lines of hydrogen by several orders of magnitude, due to the much lower abundances of those elements.

The energy e_{ijl} emitted per unit time in a line l due to the recombination of the ion j of an element X^i can be written as

$$e_{ijl} = n_e n(X_i^j) e^0_{ijl} T_e^{-\alpha}, \tag{1.1}$$

where e^0_{ijl} is a constant and the exponent α is of the order of 1. Thus, recombination line intensities increase with decreasing temperature, as might be expected.

1.2.1.2 Collisional excitation

Collisions with thermal electrons lead to excitation onto levels that are low enough to be attained. Because the lowest-lying level of hydrogen is at 10.2 eV, collisional excitation of hydrogen lines is effective only at electron temperatures T_e larger than $\sim 2 \times 10^4$ K. On the other hand, heavy elements such as nitrogen, oxygen and neon have low-lying levels that correspond to fine-structure splitting of the ground level. Those can be excited at any temperature that can be encountered in a nebula, giving rise to infrared lines.

At "typical" nebular temperatures of 8000 − 12 000 K, levels with excitation energies of a few eV can also be excited, giving rise to optical lines. Slightly higher temperatures are needed to excite levels corresponding to ultraviolet lines.

In the simple two-level approximation, when each excitation is followed by a radiative de-excitation, the energy e_{ijl} emitted per unit time in a line l due to collisional excitation of an ion j of an element X^i can be written as

$$\begin{aligned} e_{ijl} &= n_e n(X_i^j) q_{ijl} h\nu_l \\ &= 8.63 \times 10^{-6} n_e n(X_i^j) \Omega_{ijl} / (\omega_{ijl} T_e^{-0.5} e^{(\chi_{ijl}/kT_e)} h\nu_l), \end{aligned} \tag{1.2}$$

where Ω_{ijl} is the collision strength, ω_{ijl} is the statistical weight of the upper level and χ_{ijl} is the excitation energy.

Collisionally excited lines (CELs) are traditionally separated into forbidden, semi-forbidden and permitted lines, according to the type of electronic transition involved. Observable forbidden lines have transition probabilities of the order of $10^{-2}\,\mathrm{s}^{-1}$ (or less for infrared lines), semi-forbidden lines have probabilities of the order of $10^2\,\mathrm{s}^{-1}$, and permitted lines have probabilities of the order of $10^8\,\mathrm{s}^{-1}$. This means that the critical density (i.e. the density at which the collisional and radiative de-excitation rates are equal) of forbidden lines is much smaller than those of intercombination lines and of permitted lines. Table 2 of Rubin (1989) lists critical densities for optical and infrared lines. Table 1 of Hamman *et al.* (2001) gives critical densities for ultraviolet lines.

Resonance lines are special cases of permitted lines: they are the longest-wavelength lines arising from ground levels. Examples of resonance lines are H Lyα and C IV λ1550.

1.2.1.3 *Fluorescent excitation*

Permitted lines can also be produced by photoexcitation due to stellar light or to nebular recombination lines. The Bowen lines (Bowen 1934) are a particular case of fluorescence, where O III is excited by the He II Lyα line and returns to the ground level by cascades giving rise to O III λ3133, 3444 as well as to the line O III λ304, which in turn excites a term of N III.

The interpretation of fluorescence lines is complex, and such lines are not often used for diagnostics of the nebulae or their ionizing radiation. On the other hand, it is important to know which lines can be affected by fluorescence, in order to avoid improper diagnostics assuming pure recombination (see Escalante & Morisset 2005). Order-of-magnitude estimates can be made with the simple approach of Grandi (1976).

Quantitative analysis of fluorescence lines requires heavy modelling. It can be used to probe the He II radiation field in nebulae (Kastner & Bhatia 1990). The X-ray-fluorescence iron line has been used to probe accretion flows very close to massive black holes (Fabian *et al.* 2000).

1.2.1.4 *Some hints*

Each line can be produced by several processes, but usually there is one that dominates. There are, however, cases in which secondary processes may not be ignored. For example, the contribution of collisional excitation to H Lyα is far from negligible at temperatures of the order of 2×10^4 K. The contribution of recombination to the intensities of [O II] $\lambda\lambda$7320, 7330 is quite important at low temperatures (below, say, 5000 K) and becomes dominant at the lowest temperatures expected in H II regions (see Stasińska 2005).

In the appendix, we give tables of forbidden, semi-forbidden and resonance lines for ions of C, N, O, Ne, S, Cl and Ar that can be observed in H II regions and planetary nebulae.

These are extracted from the atomic-line list maintained by Peter van Hoof, which is available at http://www.pa.uky.edu/~peter/atomic. This database contains identification of about one million allowed, intercombination and forbidden atomic transitions with wavelengths in the range from 0.5 Å to 1000 µm.

W. C. Martin and W. L. Wiese produced a very useful atomic physics "compendium of basic ideas, data, notations and formulae" that is available at: http://www.physics.nist.gov/Pubs/AtSpec/index.html.

1.2.1.5 Atomic data

In the interpretation of emission lines, atomic data play a crucial role. Enormous progress has been made in atomic physics during recent years, but not all relevant data are available yet or known with sufficient accuracy. The review by Kallman & Palmeri (2007) is the most-recent critical compilation of atomic data for emission-line analysis and photoionization modelling of X-ray plasmas. A recent assessment of atomic data for planetary nebulae is given by Bautista (2006).

Many atomic databases are available on the Internet.

- A compilation of databases for atomic and plasma physics: http://plasma-gate.weizmann.ac.il/DBfAPP.html.
- Reference data: http://physics.nist.gov/PhysRefData/~physical.
- Ultraviolet and X-ray radiation at: http://www.arcetri.astro.it/science/chianti/chianti.html.
- Atomic data for astrophysics (but only up to 2000): http://www.pa.uky.edu/~verner/atom.html.
- Atomic data from the Opacity Project: http://cdsweb.u-strasbg.fr/topbase/topbase.html.
- Atomic data from the IRON project: http://cdsweb.u-strasbg.fr/tipbase/home.html.

1.2.2 *The transfer of radiation*

This section is not to provide a detailed description of radiative-transfer techniques, but simply to mention the problems and the reliability of the methods that are used.

1.2.2.1 The transfer of Lyman-continuum photons emitted by the ionizing source

The photons emitted by a source of radiation experience geometrical dilution as they leave the source. They may be absorbed on their way by gas particles, predominantly by hydrogen and helium. The first photons to be absorbed are those which have energies slightly above the ionization threshold, due to the strong dependence of the photoionization cross section on frequency (roughly proportional to ν^{-3}). This gives rise to a "hardening" of the radiation field as one approaches the outer edge of an ionized nebula. Photons may also be absorbed (and scattered) by dust grains.

1.2.2.2 The transfer of the ionizing photons produced by the nebula

Recombination produces photons that can in turn ionize the nebular gas. These photons are emitted in all directions, so their transfer is not simple. Authors have developed several kinds of approximation to deal with this.

The "on-the-spot approximation" (or OTS) assumes that all the photons recombining to the ground state are reabsorbed immediately and at the locus of emission. This is approximately true far from the ionizing source, where the population of neutral species is sufficiently large to ensure immediate reabsorption. However, in the zones of high ionization (or high "excitation" as is often improperly said), this is not true. Computationally, the OTS assumption allows one simply to discount all the recombinations to the excited levels. This creates a spurious temperature structure in the nebula, with the temperature being overestimated in the high-excitation zone, due to the fact that the stellar ionizing radiation field is "harder" than the combined stellar plus recombination radiation field. The effect is not negligible, about 1000–2000 K in nebulae of solar chemical composition. Because of this, for some kinds of problems it might be preferable to use a simple one-dimensional (1D) photoionization code with reasonable treatment of the diffuse radiation rather than a 3D code using the OTS approximation.

The OTS approximation, however, has its utility in dynamical simulations incorporating radiation transfer, because it significantly decreases the computational time.

Note that the OTS approximation is valid on a global scale. In the integrated volume of a Strömgren sphere, the total number of ionizing photons of the source is exactly balanced by the total number of recombinations to excited levels. This is a useful property for analytic estimations, since it implies that the total Hα luminosity of a nebula that absorbs all the ionizing photons (and is devoid of dust) is simply proportional to $Q_{\rm H}$, the total number of ionizing hydrogen photons.†

In increasing order of accuracy (and complexity), then comes the "outward-only approximation", which was first proposed in 1967 by Tarter in his thesis, very early in the era of photoionization codes (see Tarter *et al.* (1969) for a brief description). Here, the ionizing radiation produced in the nebula is computed at every step, but artificially concentrated in the outward-directed hemisphere, where it is distributed isotropically. This gives a relatively accurate description of the nebular ionizing radiation field, since photons that are emitted inwards tend to travel without being absorbed until they reach the symmetrical point relative to the central source. The great advantage of this approximation is that it allows the computation of a model without having to iterate over the entire volume of the nebula. The code PHOTO, used by Stasińska, and the code NEBU, used by Péquignot and by Morisset, are based on this approximation. The code CLOUDY, by Ferland, uses the outward-only approximation in a radial-only mode. It appears, from comparisons of benchmark models (e.g. Péquignot *et al.* 2001), that the global results of models constructed with codes that treat the transfer of diffuse radiation completely (e.g. the code NEBULA by Rubin) are quite similar. Note that the full outward-only approximation allows one to compute the ionizing radiation field in the shadows from optically thick clumps by artificially suppressing the stellar radiation field blocked by the clump.

Codes treating the transfer of ionizing continuum photons exactly, iterating over the entire nebula, interestingly appeared also at the beginning of the era of photoionization codes (Harrington 1968, Rubin 1968). At that time, computers were slow and had little memory, and only spherical or plane-parallel geometries could be treated by such codes.

With the present computational capacities, one can do much better and treat the transfer problem accurately for any geometry, by using Monte Carlo methods. The first such code is MOCASSIN, by Ercolano (see Ercolano *et al.* 2003). One advantage of Monte Carlo methods is that they allow one to treat the transfer accurately also in extremely dusty nebulae (Ercolano *et al.* 2005), while the outward-only approximation breaks down in such cases.

† This property is formally true only for a pure-hydrogen nebula, but it so happens that absorption by helium and subsequent recombination produces line photons that ionize hydrogen and compensate rather well for the photons absorbed by helium.

The transfer of resonance-line radiation produced in the nebula is the most difficult to treat accurately, at least in classical approaches to the transfer. This is because it is generally treated in the "escape-probability" approximation. The effect of line transfer is crucial in optically thick X-ray plasmas such as the central regions of active galactic nuclei (AGNs). The code TITAN by Dumont treats the transfer of line radiation in an "exact" manner, using the "accelerated lambda iteration" method (Dumont *et al.* 2003).

1.2.2.3 The non-ionizing lines emitted by the nebula

In general, non-ionizing photons in dust-free nebulae escape as soon as they have been emitted (except perhaps in AGNs, where column densities are higher). Resonance lines constitute an exception: they may be trapped a long time in the nebula, due to multiple scattering by atoms that, under nebular conditions, are predominantly in their ground levels.

In dusty objects, line photons suffer absorption and scattering by dust grains on their path out of the nebula. Resonance lines, whose path length can be multiplied by enormous factors due to atomic scattering, are then preferentially affected by dust extinction. Their observed luminosities then represent only a lower limit to the total energy produced by these lines.

Another case where the diagnostic potential is expected to be reduced due to transfer effects is that of infrared fine-structure lines of abundant ions, such as [O III] λ88, 52 μm, which can become optically thick in massive H II regions (Rubin 1978). However, due to a combination of independent reasons, this appears not to be the case even in the extreme situations explored by Abel *et al.* (2003).

1.3. Empirical diagnostics based on emission lines

1.3.1 *Electron temperature and density*

It is well known, and mentioned in all textbooks, that some line ratios (e.g. the ratios of the lines labelled A1 and N2 in Table 1.11 in the appendix) are strongly dependent on the temperature, since they have different excitation energies. If the critical densities for collisional de-excitations are larger than the density in the medium under study, these line ratios depend only on the temperature and are ideal temperature indicators. The most frequently used is the [O III] λ4363/5007 ratio.

On the other hand, in collisionally excited lines that arise from levels of similar excitation energies, their ratios depend only on the density. The commonest density indicator in the optical is the [S II] λ6716/6731 ratio. Other ones can easily be found by browsing in Table 1.11. Rubin (1989) gives a convenient list of optical and infrared line-density indicators showing the density range where each of them is useful.

Similar plasma diagnostics are now available in the X-ray region (Porquet & Dubau 2000, Delahaye *et al.* 2006, see also Porter & Ferland 2006).

1.3.2 *Ionic and elemental abundances*

There are basically four methods to derive the chemical composition of ionized nebulae. The first one, generally thought to be the "royal way", is through tailored photoionization modelling. The second is by comparison of given objects with a grid of models. These two methods will be discussed in the next section. In this section, which deals with purely empirical methods, we will discuss the other two: direct methods, which obtain an abundance using information directly from the spectra, and statistical methods, which use relations obtained from families of objects.

1.3.2.1 Direct methods

In these methods, one first derives *ionic* abundance ratios directly from observed line ratios of the relevant ions:

$$\frac{I_{ijl}}{I_{i'j'l'}} = \frac{\int n(\mathrm{X}_i^j) n_\mathrm{e} \epsilon_{ijl}(T_\mathrm{e}, n_\mathrm{e}) \mathrm{d}V}{\int n(\mathrm{X}_{i'}^{j'}) n_\mathrm{e} \epsilon_{i'j'l'}(T_\mathrm{e}, n_\mathrm{e}) \mathrm{d}V}, \tag{1.3}$$

where the Is are the intensities and the ϵs are given by $e_{ijl} = \epsilon_{ijl} n(\mathrm{X}_i^j) n_\mathrm{e}$.

Therefore

$$\frac{\int n(\mathrm{X}_i^j) n_\mathrm{e}\, \mathrm{d}V}{\int n(\mathrm{X}_{i'}^{j'}) n_\mathrm{e}\, \mathrm{d}V} = \frac{I_{ijl}/I_{i'j'l'}}{\epsilon_{ijl}(T_l, n_l)/\epsilon_{i'j'l'}(T_{l'}, n_{l'})}, \tag{1.4}$$

where T_l and n_l are, respectively, the electron temperature and density representative of the emission of the line l.

Assuming that the chemical composition is uniform in the nebula, one obtains the element abundance ratios:

$$\frac{n(\mathrm{X}_i)}{n(\mathrm{X}_{i'})} = \frac{I_{ijl}/I_{i'j'l'}}{\epsilon_{ijl}(T_l, n_l)/\epsilon_{i'j'l'}(T_{l'}, n_{l'})} \mathrm{ICF}, \tag{1.5}$$

where ICF is the ionization correction factor,

$$\mathrm{ICF} = \frac{\int n(\mathrm{X}_i^j)/n(\mathrm{X}_i) n_\mathrm{e}\, \mathrm{d}V}{\int n(\mathrm{X}_{i'}^{j'})/n(\mathrm{X}_{i'}) n_\mathrm{e}\, \mathrm{d}V}. \tag{1.6}$$

In a case where several ions of the same element are observed, one can use a "global" ICF adapted to the ions that are observed (e.g. $\mathrm{ICF}(\mathrm{O}^+ + \mathrm{O}^{++})$ for planetary nebulae in which oxygen may be found in higher ionization states). Note that in H II regions (except those ionized by hot Wolf–Rayet stars) $\mathrm{ICF}(\mathrm{O}^+ + \mathrm{O}^{++}) = 1$.

The application of direct methods requires a correct evaluation of the T_ls and n_ls as well as a good estimate of the ionization correction factor.

For some ions, the T_ls can be obtained from emission-line ratios such as [O III] λ4363/5007 and [N II] λ5755/6584. For the remaining ions, the T_ls are derived using empirical relations with T(4363/5007) or T(5755/6584) obtained from grids of photoionization models. The most-popular empirical relations are those listed by Garnett (1992). A newer set of relations, based on a grid of models that reproduces the properties of H II galaxies, is given by Izotov *et al.* (2006). It must be noted, however, that observations show larger dispersion about those relations than predicted by photoionization models. It is not clear whether this is due to underestimated observational error bars, or to additional processes not taken into account by photoionization models. At high metallicities,[†] the relevance of any empirical relation among the various T_ls is even more questionable, due to the existence of large temperature gradients in the nebulae, which are strongly dependent on the physical conditions.

[†] Throughout, the word "metallicity" is used with the meaning of "oxygen abundance". This is common practice in nebular studies. Although oxygen is not a metal according to the definition given by chemistry, in nebular astronomy the word metal is often used to refer to any element with relative atomic mass ≥12. The use of the O/H abundance ratio to represent the "metallicity" – as was first done by Peimbert (1978) – can be justified by the facts that oxygen represents about half of the total mass of the "metals" and that it is the major actor – after hydrogen and helium – in the emission spectra of nebulae. Note that, for stellar astronomers, the word "metallicity" is related to the iron abundance, rather than to the oxygen abundance, so the two uses of the word "metallicity" are not strictly compatible, since the O/Fe ratio changes during the course of chemical evolution.

Cambridge University Press
978-0-521-89886-7 - The Emission-Line Universe: XVIII Canary Islands Winter School of Astrophysics
Edited by Jordi Cepa
Excerpt
More information

The ionization correction factors that are used are based either on ionization potential considerations or on formulae obtained from grids of photoionization models. For H II galaxies, a set of ICFs is given by Izotov *et al.* (2006). For planetary nebulae, a popular set of ionization correction factors is that from Kingsburgh & Barlow (1994), which is based on a handful of unpublished photoionization models. Stasińska (2007, in preparation) gives a set of ICFs for planetary nebulae based on a full grid of photoionization models. It must be noted, however, that theoretical ICFs depend on the model stellar atmospheres that are used in the photoionization models. Despite the tremendous progress in the modelling of stellar atmospheres in recent years, it is not yet clear whether predicted spectral energy distributions (SEDs) in the Lyman continuum are correct.

Finally, note that the line-of-sight ionization structure, in the case of observations that sample only a small fraction of the entire nebula, is different from the integrated ionization structure. This is especially important to keep in mind when dealing with trace ionization stages.

A case of failure of $T_{\rm e}$-based abundances: metal-rich giant H II regions. Until recently, it was not possible to measure the electron temperature in metal-rich H II regions. The usual temperature diagnostics involve weak auroral lines, which easily fall below the detection threshold at low temperatures. With very large telescopes, such temperature-sensitive line ratios as [O III] λ4363/5007, [N II] λ5755/6584 and [S III] λ6312/9532 can now be measured even at high metallicities (e.g. Kennicutt *et al.* 2003, Bresolin *et al.* 2005, Bresolin 2007). However, due to the large temperature gradients expected to occur in high-metallicity nebulae, which are a consequence of the extremely efficient cooling in the O^{++} zone due to the infrared [O III] lines, [O III] λ4363/5007 does not represent the temperatures of the O^{++} zone. As a consequence, the derived abundances can be strongly biased, as shown by Stasińska (2005). The magnitude of the bias depends on the physical properties of the H II region and on which observational temperature indicators are available.

A further problem in the estimation of $T_{\rm e}$ at high metallicity is the contribution of recombination to the intensities of collisionally excited lines, which becomes important at low values of $T_{\rm e}$. For example, the contribution of recombination from O^{++} to the intensity of [O II] can be very important. It can be corrected for by using the formula given in Liu *et al.* (2000), provided that the temperature characteristic of the emission of the recombination line is known. If the temperature is measured using ratios of CELs only, that is not the case.

1.3.2.2 Statistical methods

In many cases, the weak [O III] λ4363 or [N II] λ5755 lines are not available because either the temperature is too low or the spectra are of low signal-to-noise ratio, or else the data consist of narrow-band images in the strongest lines only. Then, one may use the so-called "strong-line methods" to derive abundances. Such methods are only statistical, in the sense that they allow one to derive the metallicity of an H II region only on the assumption that this H II region shares the same properties as those of the H II regions used to calibrate the method. In practice, such methods work rather well for giant H II regions, since it appears that giant H II regions form a narrow sequence (see e.g. McCall *et al.* 1985), in which the hardness of the ionizing radiation field and the ionization parameter are closely linked to the metallicity. Indeed, an increased metallicity enhances the metal line blocking of the emergent stellar flux in the extreme ultraviolet and softens the ionizing spectrum. In addition, the pressure exerted on the nebular gas increases with the strength of the stellar winds, which are related to metallicity, and this in turn decreases the ionization parameter (Dopita *et al.* 2006).

Unlike direct methods for abundance determinations, statistical methods have to be calibrated. The reliability of these methods depends not only on the choice of an adequate indicator, but also on the quality of the calibration. This calibration can be done using grids of ab-initio photoionization models (McGaugh 1991), using a few tailored photoionization models (Pagel *et al.* 1979), abundances derived from direct methods (Pilyugin & Thuan 2005), or objects other than H II regions thought to have the same chemical composition (Pilyugin 2003).

The oldest and still most-popular statistical method is the one based on oxygen lines. Pagel *et al.* (1979) introduced the ([O II] λ3727 + [O III] λ4959,5007)/Hβ ratio (later referred to as R_{23} or O_{23}) to estimate O/H. This method has been calibrated many times, with results that may differ by about 0.5 dex. McGaugh (1994) and later Pilyugin (2000, 2001) refined the method to account for the ionization parameter.

Many other metallicity indicators have been proposed: [O III] λ5007/[N II] λ6584 (O_3N_2) by Alloin *et al.* (1979); [N II] λ6584/Hβ (N_2), by Storchi-Bergmann *et al.* (1994); ([S III] λ9069 + [S II] λ6716, 6731)/Hα (S_{23}) by Vílchez & Esteban (1996); [N II] λ6584/[O II] λ3727 (N_2O_2) by Dopita *et al.* (2000); [Ar III] λ7135/[O III] λ5007 (Ar_3O_3) and [S III] λ9069/[O III] λ3869 (S_3O_3) by Stasińska (2006); and [Ne III] λ9069/[O II] λ3727 (Ne_3O_2) by Nagao *et al.* (2006). The metallicity indicators proposed until 2000 have been compared by Pérez-Montero & Díaz (2005). However, all those methods will have to be recalibrated when the emission-line properties of the most-metal-rich H II regions are well understood, which is not the case at present.

A few comments are in order. First, any method based on the ratio of an optical CEL and a recombination line (e.g. O_{23} or S_{23}) is bound to be double-valued, as illustrated e.g. by Figure 7 of Stasińska (2002). This is because, at low metallicities, such ratios increase with increasing metallicity, whereas at high metallicities they decrease with increasing metallicity due to the greater cooling by infrared lines, which lowers the temperature below the excitation threshold of optical CELs. In such circumstances, external arguments must be relied upon to find out whether the object under study is on the "high-abundance" or "low-abundance" branch. The commonest argument is based on the [N II] λ6584 line. The reason why this argument works is that the N/O ratio is observed to increase as O/H increases, at least at high metallicities. Besides, high-metallicity H II regions tend to have lower ionization parameters, favouring low-excitation lines such as [N II] λ6584. The biggest problem is at intermediate metallicities, where the maxima of O_{23} and S_{23} occur and the metallicity is very ill-determined. By using both O_{23} and S_{23} indices at the same time, it would perhaps be possible to reduce the uncertainty.

Methods that use the [N II] λ6584 lines have another potential difficulty. The chemical evolution of galaxies changes the N/O ratio in a complicated and non-universal way. Therefore, a calibration is not necessarily relevant for the group of objects under study.

Perhaps the most satisfactory methods, on the theoretical side, are the ones using the Ar_3O_3 or S_3O_3 indicators, since these indicators are monotonic and work for well-understood reasons, which are directly linked to metallicity.

Conversely, the Ne_3O_2 index, which is seen to decrease as metallicity decreases, behaves in such a way *only* because metal-richer giant H II regions happen to be excited by a softer radiation field and have a lower ionization parameter. This is a very indirect metallicity indicator!

It is important to be aware that, in principle, strong-line methods can be safely used only when applied to the same category of objects as was used for the calibration. The meaning of the results in the case of integrated spectra of galaxies, for example, is far from

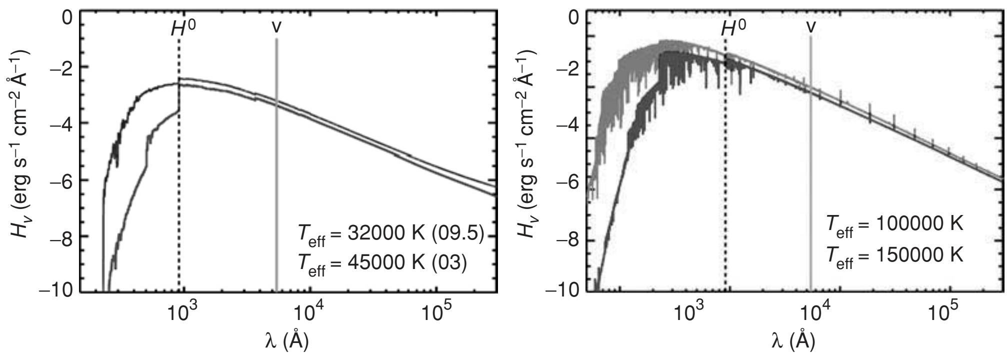

FIGURE 1.1. Spectral energy distributions (SEDs) for effective temperatures corresponding to massive stars (left) and central stars of planetary nebulae (right). The dotted line indicates the position of the ionization potential of hydrogen; the full line indicates the wavelength of the V filter.

obvious in an absolute sense. Such spectra contain the light from H II regions differing in chemical composition and extinction as well as the light from the diffuse ionized interstellar medium. In addition, inclination effects may be important. A few studies have addressed these issues from an observational point of view (Zaritsky *et al.* 1994, Kobulnicky *et al.* 1999, Moustakas & Kennicutt 2006), but clearly the subject is not closed.

A further step in strong-line abundance determinations has been made by using ratios of line equivalent widths (EWs) instead of intensities (Kobulnicky *et al.* 2003). The advantage of using equivalent widths is that they are almost insensitive to interstellar reddening, which allows one to apply the method even when reddening corrections are not available, especially at redshifts larger than 1.6. The reason why equivalent widths work well for integrated spectra of galaxies is that there is empirically a very close correlation between line intensities and equivalent widths, meaning that, statistically, stellar and nebular properties as well as the reddening are closely interrelated.

1.3.3 *Estimation of the effective temperature of the ionizing stars*

$T_\star$ from the Zanstra method. This method, proposed by Zanstra (1931), makes use of the fact that the number of stellar quanta in the Lyman continuum, normalized with respect to the stellar luminosity at a given wavelength, is an increasing function of the effective temperature. This is illustrated in Figure 1.1 (based on modern stellar model atmospheres). In practice, it is the luminosity of the Hβ line which is the counter of Lyman-continuum photons. This assumes that all the Lyman-continuum photons are absorbed by hydrogen. This assumption breaks down in the case of density-bounded nebulae or of nebulae containing dust mixed with the ionized gas. In real nebulae, some Lyman-continuum photons are also absorbed by He^0 and He^+. However, recombination of these ions produces photons that are able to ionize hydrogen, so the basic assumption of the Zanstra method is generally remarkably well fulfilled. Of course, the value of the effective temperature, $T_\star$, obtained by the Zanstra method will depend on the model atmosphere used in the derivation.

For very hot stars, such as the central stars of planetary nebulae, one can also define a He^+ Zanstra temperature, using the He II λ4686 flux as a measure of the number of photons with energies above 54.4 eV.